

# TDAN: Top-Down Attention Networks for Enhanced Feature Selectivity in CNNs

Shantanu Jaiswal  
A\*STAR AI Initiative  
jaiswals@ihpc.a-star.edu.sg

Basura Fernando  
A\*STAR AI Initiative

Cheston Tan  
A\*STAR AI Initiative

## Abstract

Attention modules for Convolutional Neural Networks (CNNs) are an effective method to enhance performance of networks on multiple computer-vision tasks. While many works focus on building more effective modules through appropriate modelling of channel-, spatial- and self-attention, they primarily operate in a feedforward manner. Consequently, the attention mechanism strongly depends on the representational capacity of a single input feature activation, and can benefit from incorporation of semantically-rich higher-level activations that can specify “what and where to look” through top-down information flow. Such feedback connections are also prevalent in the primate visual cortex and recognized by neuroscientists as a key component in primate visual attention.

Accordingly, in this work, we propose a lightweight top-down (TD) attention module that iteratively generates a “visual searchlight” to perform top-down channel and spatial modulation of its inputs and consequently outputs more selective feature activations at each computation step. Our experiments indicate that integrating TD in CNNs enhances their performance on ImageNet-1k classification and outperforms prominent attention modules while being more parameter and memory efficient. Further, our models are more robust to changes in input resolution during inference and learn to “shift attention” by localizing individual objects or features at each computation step without any explicit supervision. This capability results in 5% improvement for ResNet50 on weakly-supervised object localization besides improvements in fine-grained and multi-label classification.

## 1. Introduction

The design and incorporation of attention modules in deep CNNs has gained considerable recognition in computer vision due to their ability to enhance the representation power and performance of these networks in a task-agnostic manner. These modules typically formulate atten-

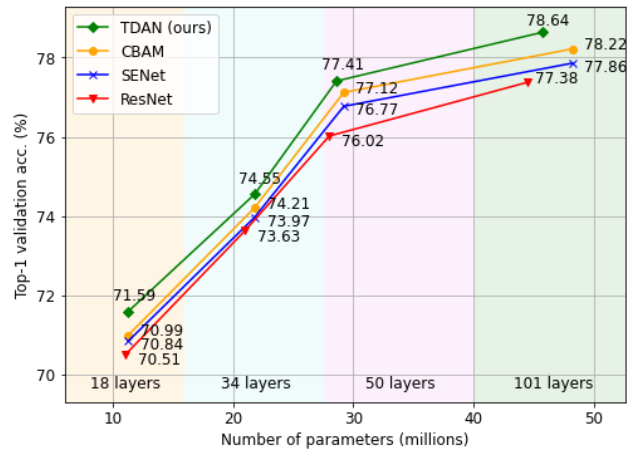


Figure 1. ImageNet-1k classification performance on 224 x 224 input resolution for ResNet [13] backbones. TDAN outperforms popular attention modules SE [16] and CBAM [37] and requires lesser parameters and is faster to train as models grow deeper.

tion as a mechanism of feature modulation in outputs of traditional convolutional blocks by learning to intensify activations for deemed salient features and suppress activations for irrelevant ones. As a prominent method, Squeeze & Excitation (SE) [16] introduces channel attention modelling of global-average-pooled (GAP) feature representations, which is then enhanced by CBAM [37] through additional incorporation of spatial attention and utilization of both global-max-pooled (GMP) and GAP representations. Further, recent works [12, 27, 35] identify how channel attention can be made more efficient and effective, while a different direction of work augments convolutional operations with self-attention and calibration methods [3, 22] to learn more effective feature representations.

However, conventional attention modules predominantly operate in a feedforward manner, i.e. they only utilize the output feature map of a convolutional block to both determine attention weights and perform attention modulation. As a result, the attentional mechanism is constrained to the representational capacity and local information of a single feature representation, and can benefit from incorporat-

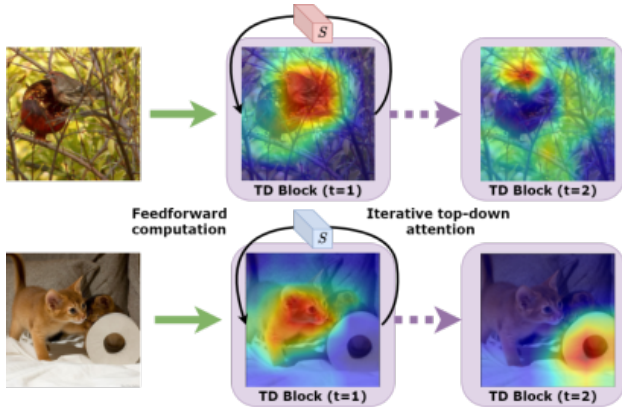


Figure 2. Illustration of how iterative top-down feedback computation can help increase feature selectivity and thereby process individual salient features or objects at each computation step. Green arrows indicate feedforward inputs to TD blocks and red dotted arrows indicate top-down computation within TD block.

ing semantically-rich contextual information available at higher-level feature representations. This can be effectively facilitated by introducing a top-down feedback operation between higher-level and lower-level feature representations within a convolutional block. Hence, in this work, we explore how top-down feedback computation can be effectively modelled to obtain more selective and contextually-informed feature activations across the CNN hierarchy.

**Designing a top-down attention module with visual searchlights for feature attention.** A foundational formulation of top-down computation during visual processing was introduced by Crick in his “searchlight hypothesis” [9], where he postulated the presence of an internal “attentional searchlight” in the brain that operates by iteratively selecting lower-level neurons to “co-fire” with semantically richer higher-level neurons, such that at any given instance, a sparse and strongly correlated set of selected lower and higher-level neurons fired together. Taking inspiration from his hypothesis, we propose a novel top-down (TD) attention module that jointly models constituent higher-level and lower-level features to obtain a “visual searchlight” [9, 33] that carries information on which lower-level features are of interest for subsequent computation. This searchlight then does attentional modulation of lower-level features by first performing channel attention through conventional channel scaling (“highlighting features of interest”) and then performing spatial scaling (“intensifying spatial locations of highlighted features”) by applying a spatial map obtained through its utilization in a single pointwise convolution.

**Our proposed module is lightweight (in terms of parameters) and can be conveniently integrated** at multiple levels of the CNN hierarchy as a standard plug-in attention module and trained end-to-end with standard backpropaga-

tion. We discuss more details of our approach in section 3, and here briefly indicate two distinct advantages of the described operation of the visual searchlight – (i) it enables selective activation of features at each computation step allowing it to localize and process individual features at each step (ii) it is more robust in performing spatial attention at changing input resolutions [32] in comparison to static convolutional kernel-based attention methods [30, 37].

**Contributions:** (i) We introduce a novel lightweight top-down attention module for CNNs by incorporating appropriate computational and neuroscience motivations in its design. (ii) We show the effectiveness of our module in enhancing performance of mainstream CNN models (ResNet and MobileNetV3), outperforming state-of-the-art attention modules across multiple object recognition benchmarks, besides performing extensive ablation analysis to highlight key factors influencing the module’s performance. (iii) We demonstrate how our proposed module makes CNNs more robust to input resolution changes during inference and enables the emergent property of “attention-shifting” through appropriate qualitative and quantitative analyses.

## 2. Related work

### 2.1. Attention modules for CNNs

Initial work in the design of attention modules for CNNs includes the proposal of stacked attention modules for residual networks [34] and SE’s [16] channel attention formulation for feature aggregation and recalibration of GAP representations through fully connected layers. As extensions to SE, many works have focused on how to enhance the feature aggregation process by incorporating spatial and graph operations and more effective methods to estimate channel interactions than GAP. GE [15] introduces a spatial gather-excite operator to augment channel attention, GSoP proposes second-order global pooling methods [12], C3 [39] incorporates graph convolutional networks for channel interactions and  $A^2$ -Nets [8] incorporate second-order attentional pooling for long-range dependencies in image/video recognition. Notably, CBAM [37] along with [24, 30] demonstrate the advantage of incorporating spatial attention in conjunction to channel attention, while CBAM also indicates effectiveness of using GMP and GAP for feature aggregation. Further, AANets [3] and SCNet [22] demonstrate how self-attention and self-calibration operations can augment standard convolutions, while GCNet [6] extends non-local neural networks to augment SE operations. More recently, prominent modules include ECA [35] which proposes one-dimensional convolutions to efficiently capture inter-channel interactions for channel attention and FCA [27] which proposes utilization of discrete cosine transform based frequency compression methods to effectively perform feature aggregation in SE in place of GAP.

## 2.2. Top-down feedback computation in CNNs

Integrating top-down feedback computation in CNNs has in general been shown to improve performance on a variety of computer vision tasks. For instance, in neural image captioning and visual question answering, multiple methods employ variants of recurrent neural networks (RNNs) along with visual features from a CNN in an encoder-decoder setup [1, 7, 38, 40]. Similarly, RNNs have also been proposed to model visual attention for context-driven sequential computation in scene labelling [4, 26], object recognition [41, 43] and “glimpse” based processing [2, 23] for multi-object classification. Finally, approaches also model top-down feedback to iteratively localize salient features [11], keypoints [17] or objects [5] and improve performance for fine-grained classification and object classification with cluttered inputs. While these approaches propose novel top-down feedback formulations, they are specifically formulated for target tasks and applied on top of existing ImageNet-1k pretrained backbone CNN models. In contrast, our top-down formulation serves a more general function of contextually-informed feature modulation of intermediate features across the CNN hierarchy and is integrated internally as a standard plug-in attention module trained with standard backpropagation.

## 3. Top-down (TD) attention module

We are given a convolutional block  $\mathbf{B}$  comprising of  $N$  convolutional layers, each denoted by  $\mathbf{L}_n$  where  $n \in \{1..N\}$ , that maps an input feature map  $\mathbf{X}^0 \in \mathbb{R}^{C_0 \times H_0 \times W_0}$  to an output feature map  $\mathbf{X}^N \in \mathbb{R}^{C_N \times H_N \times W_N}$  through feedforward operation denoted by  $\mathbf{L}_N(\mathbf{L}_{N-1}..(\mathbf{L}_1(\mathbf{X}^0)))$ . We denote the output of the top-down feedback operation in the block  $\mathbf{B}$  for a given  $t$  number of computational steps by  $\mathbf{X}_t^N$  where  $t \in \{1..T\}$ . Similarly,  $\mathbf{X}_t^0$  is the input at computational step  $t$ . We infer a 1D attentional searchlight  $\mathcal{S}_t \in \mathbb{R}^{C_0 \times 1 \times 1}$  that is used to sequentially perform channel and spatial attention of  $\mathbf{X}_t^0$  to obtain the next computational step input  $\mathbf{X}_{t+1}^0$ , which is subsequently feedforwarded to obtain  $\mathbf{X}_{t+1}^N$  as illustrated in figure 3. The operations for each computational step  $t$  can be summarized as follows:

$$\mathbf{X}_t^N = \mathbf{L}_N(\mathbf{L}_{N-1}..(\mathbf{L}_1(\mathbf{X}_t^0))) \quad (1)$$

$$\mathcal{S}_t = \begin{cases} \mathbf{g}(\mathbf{X}_t^N, \mathbf{X}_t^0) & \text{if joint attention} \\ \mathbf{g}(\mathbf{X}_t^N) & \text{if top attention} \end{cases} \quad (2)$$

$$\mathbf{X}_{t+1}^0 = \text{att}(\mathbf{X}_t^0; \mathcal{S}_t) \quad (3)$$

where  $\mathbf{g}(\cdot)$  is a learnable transformation and  $\text{att}(\cdot)$  denotes channel and spatial attention. We provide more details for both below. The computation is repeated for  $T$  computational steps and the final output of the block is  $\mathbf{X}_T^N$ .

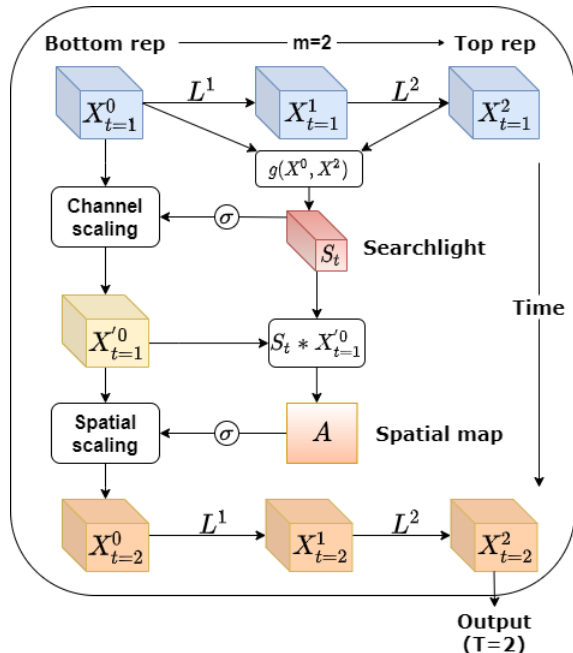


Figure 3. **Overview of our proposed top-down attention module** with “joint” bottom and top attention (eq. 4). Given an input bottom feature map and feedforwarded top feature map, an “attentional searchlight”  $\mathcal{S}_t$  is inferred to perform channel and spatial attention of the existing input to obtain its next computational step representation, which is subsequently feedforwarded. This is repeated for  $T$  computational steps to obtain the final output  $\mathbf{X}_{t=T}^N$  ( $N$  and  $T=2$  in figure). ‘ $m$ ’ denotes the feedback distance between top and bottom representations.

**Obtaining the attentional searchlight.** In our proposed module, the attentional searchlight  $\mathcal{S}_t$  aims to specify which channels and spatial locations in a lower-level feature map should be emphasized for the next computational step and is derived from joint modelling of a higher-level feature map that captures a higher degree of semantic information [42] and lower-level feature map that contains local feature information. Hence, we model the generation of  $\mathcal{S}_t$  as a joint learnable transformation of the higher-level feature map  $\mathbf{X}_t^N$  and lower-level feature map  $\mathbf{X}_t^0$ . To perform the transformation, we first individually estimate channel activations by squeezing [16] the spatial dimensions of respective feature maps with an unparameterized pooling operation for both feature maps resulting in corresponding 1D channel vectors, for higher-level  $\in \mathbb{R}^{C_N}$  and for lower-level  $\in \mathbb{R}^{C_0}$ . These vectors are then individually passed through distinct single hidden layer multi-layer perceptrons (MLP) and subsequently concatenated and passed through another single layer MLP to obtain a target 1D vector which we coin as *Attention Searchlight* (i.e.  $\mathcal{S}_t$  given by equation 2). This computation is shown to be effective and efficient and also

allows us to perform top-down feedback independent of the channel and spatial dimensions of top and bottom feature maps (i.e.  $\mathbf{X}_t^N$  and  $\mathbf{X}_t^0$  can be of different dimensions). The specific computation to obtain *Attention Searchlight* is summarized as follows:

$$\mathcal{S}_t = \mathbf{g}(\mathbf{X}_t^N, \mathbf{X}_t^0) = \sigma(\mathbf{W}_s(\text{ReLU}[\mathbf{W}_t(\mathbf{X}_{t,p}^N); \mathbf{W}_b(\mathbf{X}_{t,p}^0)])) \quad (4)$$

where  $\mathbf{W}_t \in \mathbb{R}^{C_N/r \times C_N}$ ,  $\mathbf{W}_b \in \mathbb{R}^{C_0/r \times C_0}$  and  $\mathbf{W}_s \in \mathbb{R}^{C_0 \times (C_N + C_0)/r}$  are weights of the MLP with ReLU activation applied after  $\mathbf{W}_t$  and  $\mathbf{W}_b$ ,  $r$  is a reduction ratio to reduce parameter complexity (we use 16),  $\sigma$  is the sigmoid activation function and pooled representations are indicated by subscript  $p$ , i.e.,  $\mathbf{X}_{t,p}^N = \text{Pool}(\mathbf{X}_t^N)$  and we utilize spatial average-pooling for the  $\text{Pool}()$  operator. Accordingly, we term the formulation in eq. 4 as **joint attention** as it depends on both top and bottom feature-maps.

For cases where more parameter efficiency is desired (e.g. relatively large number of bottom channels), we model the generation of  $\mathcal{S}_t$  based on the hidden layer MLP representation of only the top feature map  $\mathbf{X}_t^N$ . We coin the below formulation as **top attention**:

$$\mathcal{S}_t = \mathbf{g}(\mathbf{X}_t^N) = \sigma(\mathbf{W}_s[\text{ReLU}(\mathbf{W}_t(\mathbf{X}_{t,p}^N))]) \quad (5)$$

where  $\mathbf{W}_t \in \mathbb{R}^{C_N/r \times C_N}$  and  $\mathbf{W}_s \in \mathbb{R}^{C_0 \times C_N/r}$  are weights of the MLP with ReLU activation applied after  $\mathbf{W}_t$ , and  $\sigma$  is the sigmoid activation function.

**Performing channel and spatial attention.** We interpret the obtained attentional searchlight  $\mathcal{S}_t$  to first be a channel attention vector signifying which channels of  $\mathbf{X}_t^0$  should be ‘‘highlighted’’ for the next computation step. Consequently, as a first step, we scale the existing representation  $\mathbf{X}_t^0$  through element-wise multiplication with  $\mathcal{S}_t$  (broadcasted spatially to match dimensions) to obtain its channel-scaled representation  $\mathbf{X}_t^{\prime 0}$ . We then perform pointwise convolution of  $\mathcal{S}_t$  and  $\mathbf{X}_t^{\prime 0}$  with  $\mathcal{S}_t$  treated as a single  $1 \times 1$  filter  $\in \mathbb{R}^{1 \times 1 \times C_0}$  to obtain a 2D spatial map  $\mathcal{A} \in \mathbb{R}^{H_0 \times W_0}$  that specifies salient spatial locations in the scaled feature map  $\mathbf{X}_t^{\prime 0}$ . Then,  $\mathbf{X}_t^{\prime 0}$  is scaled spatially through element-wise multiplication with the sigmoidal activation of  $\mathcal{A}$  (broadcasted channel-wise to match dimensions) to obtain the next computational-step input representation  $\mathbf{X}_{t+1}^0$ . We denote these set of operations as  $\text{att}(\mathbf{X}_t^0; \mathcal{S}_t)$  and summarize it as:

$$\mathbf{X}_t^{\prime 0} = \mathbf{X}_t^0 \otimes \mathcal{S}_t \quad (6)$$

$$\mathcal{A} = \mathcal{S}_t * \mathbf{X}_t^{\prime 0} \quad (7)$$

$$\mathbf{X}_{t+1}^0 = \mathbf{X}_t^{\prime 0} \otimes \sigma(\mathcal{A}) \quad (8)$$

where  $\otimes$  denotes element-wise product and  $*$  denotes pointwise convolution.

The intuition to perform pointwise convolution to obtain  $\mathcal{A}$  is that the channel weights in  $\mathcal{S}_t$  and increased activations

for selected channels in  $\mathbf{X}_t^{\prime 0}$  ensure that only those spatial locations that correspond to selected channels are activated with convolution behaving as a spatial ‘‘search’’ operation of selected lower-level features. A notable benefit of this formulation is that it can enable the model to be more robust to changes in input resolution that may occur during model inference and that can impact activation statistics of pooling layers [32] and spatial attention techniques that utilize fixed convolutional kernels [30, 37].

**Integration in existing CNN models.** As mentioned previously, our proposed module does not require the bottom input  $\mathbf{X}_t^0$  to be of the same dimensions as the top output  $\mathbf{X}_t^N$ . Hence, it can be integrated into many CNN models as a standard attention module at multiple levels of the processing hierarchy and be trained end-to-end with standard backpropagation. Further, the formulation can be generalized to be a single block spanning the entire CNN model with the bottom input  $\mathbf{X}_t^0 = \text{image input}$  and  $\mathbf{X}_t^N = \text{pre-classifier feature map}$ . However, we empirically find that having a large feedback-distance (number of feedforward convolutional layers) denoted by ‘‘ $m$ ’’ between bottom representation  $\mathbf{X}_t^0$  and the top representation  $\mathbf{X}_t^N$  leads to unstable training and significantly worsen the performance. This is possibly due to a radical shift in input distributions over computational-steps for intermediate convolutional layers (i.e. the layer receives two radically different inputs over computational-steps) due to changes accumulated over previous layer outputs that amplify with higher number of previous layers. Hence, for our experiments, we study ‘‘ $m$ ’’ between 1 to 3 within a standard convolutional block, and specifically apply multiple instantiations of the module at deeper semantically-richer [42] levels of a CNN model. Further, we use unique batch normalization layers for each computation step to stabilize training as suggested in findings of [20]. We denote our proposed top-down module which operates for  $T$  computational steps and over feedback-distance  $M$  with **TD** ( $t=T$ ,  $m=M$ ) where TD is further specified as top attention (eq. 5) or joint attention (eq. 4). An example integration of the module in a ResNet [13] block is shown in figure 4.

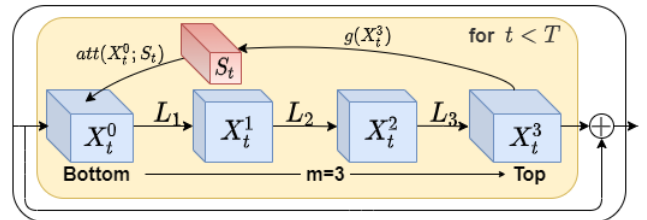


Figure 4. **Integration of top-down (TD) module using ‘‘top’’ attention (eq. 5) in a ResNet [13] bottleneck block.** As shown, TD operates before the residual connection for preset computational steps  $T$  and its output is added to the ResNet block input.

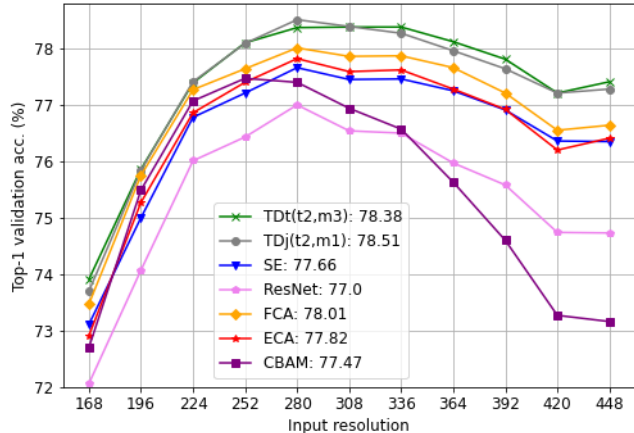


Figure 5. Performance of models (ResNet50 backbone) on ImageNet-V1 (ILSVRC-12 [10]) at different test resolutions with best accuracy reported in plot legend and table 2. TD models obtain better results at higher resolutions in comparison to baselines that fall below their original 224x224 performance.

## 4. Experimental results and discussion

We evaluate our proposed top-down (TD) attention module on the standard benchmarks: ImageNet-1k [10] for large-scale object classification and localization, CUB-200 [36] and Stanford Dogs [19] for fine-grained classification and MS-COCO [21] for multi-label image classification.

We perform experiments with two mainstream CNN model types – ResNet [13] and MobileNetV3 [14]. We compare performance with the original models and prominent attention modules including Squeeze & Excitation networks (SE) [16], CBAM [37], ECA [35] and FCA [27]. To our knowledge, FCA is the most recent attention module shown to effectively enhance performance of multiple CNN variants. For ResNet models, we apply our module at all blocks of layers 3 and 4 (with exception of ResNet101 wherein we either simply apply only at layer 4 or at layer 4 and 10 alternating blocks in layer 3 to preserve computational complexity in comparison to baselines). For MobileNetV3 large, we apply our module at the final three layers, replacing the existing SE blocks in those layers. For fair comparison, we reproduce all experiments in PyTorch [25] with the same training strategy used for all models. Training details and hyperparameter configurations for all experiments are provided in supplemental. Source code for experiments and pre-trained models will be made publicly available and is also provided in supplementary material.

### 4.1. Large-scale object classification (ImageNet-1k)

We first perform experiments on large-scale object classification with the ImageNet-1k dataset and evaluate our module on ResNet variants: ResNet18, ResNet34,

ResNet50 and ResNet101. For comprehensive evaluation, we consider two distinct validation sets – the original ILSVRC-12 validation set comprising 50,000 images [10] and the more recent ImageNet V2 [28] “top-images” set with 10,000 new images. We hereafter refer them as ImageNet-V1 and ImageNet-V2 respectively. We assess models based on their top1 and top5 single crop validation accuracy. Additionally, for models with our TD module, which output localized object predictions at each computation step (as shown in fig. 6), we only consider the most confident prediction during both training and evaluation with exception of a minority of images that comprise multiple objects, for which we consider only predictions with unique localization maps (having an IOU of  $< 0.5$ ).

We summarize our experimental results for ResNet50 and ResNet101 in table 1, and compare the top configurations of our TD module with aforementioned baselines. We find that our optimal formulation is TDjoint( $t=2, m=1$ ), which achieves a top1 accuracy of 79.80% on ImageNet-V2 and increases performance of original ResNet50 by 2.3%. It also outperforms baseline feedforward attention modules on both validation sets for both ResNet50 and ResNet101 while having lesser parameters and comparable or higher training and inference speed in most cases (with exception of ECA). For ResNet101, it achieves a 0.78% higher top1 accuracy on ImageNet-V1 in comparison to SE when applied at both layers 3 and 4. We find similar increments for TDtop( $t=2, m=1$ ), a lighter variant of our module utilizing only top attention, and TDtop( $t=2, m=3$ ), a computationally expensive variant with larger feedback distance. Our method outperforms all prior state-of-the-art methods including the recent FCA-TS [27], perhaps due to the effectiveness of top-down attention mechanism of our module. These improvements become more apparent in more challenging tasks such as weakly supervised localization as shown later.

**Computation cost comparison:** Since our modules perform iterative top-down computation, they have a higher associated number of FLOPs than existing feedforward modules. Further, the number of FLOPs grows as the feedback distance ( $m$ ) increases – growing by 20% in case of ResNet50 from  $m=1$  to  $m=3$ . However, we find that this limitation can be managed in practice during both training and inference in comparison to baseline modules since our models (specifically with  $m=1$ ) require lesser parameters and memory operations, and hence have comparable or higher FPS (speed). As shown in table 1, TD models with  $m=1$  have higher FPS than both CBAM and FCA for ResNet50, and higher FPS than SE as well for ResNet101.

### Evaluation of models at different input resolutions.

The activation statistics of the global pooling in CNNs have been shown to be strongly impacted by changes in input resolutions [32], thereby making performance of CNNs sus-

Method	Backbone	Param.	FLOPs	Mem.(Gb)		FPS/gpu		ImageNet-V2		ImageNet-V1	
				Trn	Val	Trn	Val	Top1	Top5	Top1	Top5
-	-	-	-	-	-	-	-	-	-	-	-
ResNet [13]	ResNet50	25.56 M	4.12 G	29.5	16.1	195	570	77.54	94.50	76.02	92.95
SE [16]		28.07 M	4.13 G	32.4	16.0	162	496	78.72	95.05	76.77	93.49
CBAM [37]		28.07 M	4.14 G	37.6	20.7	107	347	79.05	95.57	77.12	93.53
ECA [35]		25.56 M	4.13 G	31.5	16.1	168	502	78.64	94.95	76.86	93.34
FCA-TS [27]		28.07 M	4.13 G	32.4	16.3	146	468	79.20	95.34	77.23	93.43
TDjoint (t=2, m=1)		27.65 M	4.59 G	31.9	16.2	160	493	79.80	95.30	<b>77.41</b>	93.62
TDtop (t=2, m=1)		27.06 M	4.59 G	31.8	16.0	162	495	79.38	95.21	77.36	93.59
TDtop (t=2, m=3)		27.66 M	5.98 G	35.3	16.3	131	405	<b>79.85</b>	<b>95.59</b>	77.40	<b>93.63</b>
ResNet [13]	ResNet101	44.55 M	7.85 G	39.2	16.6	123	368	78.84	95.43	77.38	93.63
SE [16]		49.29 M	7.86 G	45.5	16.9	98	321	79.29	95.65	77.86	93.69
CBAM [37]		49.29 M	7.88 G	53.3	21.4	70	226	79.79	95.88	78.22	94.08
FCA-TS [27]		49.29 M	7.86 G	47.0	17.1	94	304	79.95	95.94	78.20	94.01
TDjoint (t=2, m=1)		46.75 M	8.37 G	41.0	16.8	105	339	80.29	<b>96.09</b>	<b>78.64</b>	<b>94.21</b>
TDjoint (t=2, m=1, L4)		45.94 M	8.01 G	40.3	16.8	113	350	<b>80.52</b>	95.91	78.22	93.99

Table 1. Top1 & Top5 single-crop classification accuracy (%) of ResNet50 and ResNet101 integrated with our TD module in comparison to baselines on original ImageNet-V1 [10] and recent ImageNet-V2 [28] validation sets. All models are reproduced and trained with same experimental setup and selected on best ImageNet-V1 performance. Further backbones and baselines in supplemental for better readability.

Model (ResNet50)	ImageNet-V1 Top1 Acc. (%)			
	Best	224 <sup>2</sup>	168 <sup>2</sup>	448 <sup>2</sup>
-	-	-	-	-
ResNet [13]	77.00	76.02	72.06	74.73
SE [16]	77.66	76.77	73.11	76.35
CBAM [37]	77.47	77.12	72.70	73.16
ECA [35]	77.82	76.86	72.91	76.41
FCA-TS [27]	78.01	77.23	73.47	76.61
TDjoint (t=2, m=1)	<b>78.51</b>	<b>77.41</b>	73.70	77.28
TDtop (t=2, m=3)	78.38	77.40	<b>73.91</b>	<b>77.41</b>

Table 2. Performance of models with ResNet50 backbone on ImageNet-V1 single crop object classification at different testing resolutions (all models were trained on 224<sup>2</sup> resolution). Most models obtain best accuracy at 280<sup>2</sup> resolution as shown in fig. 5.

ceptible to variations in input resolution. Hence, in this experiment, we study whether attention modules including TD can enhance robustness of CNNs by evaluating ResNet50 models at different resolutions for ImageNet-V1. We plot results for all models in fig. 5 for testing resolutions from 168x168 to 448x448 with increments of 28 (further lower resolutions provided in supplemental). Additionally, in table 2, we indicate each model’s performance at lowest resolution of 168x168 (denoted by 168<sup>2</sup>), performance at highest resolution of 448x448, best testing performance and original 224x224 performance.

We find that: (i) TD-models largely retain their original performance at higher resolutions, particularly obtaining a 3% better performance than the original ResNet model at 448x448. (ii) CBAM, which utilizes a fixed convolutional kernel to model spatial attention, has a significant drop in performance at higher resolutions. (iii) Other attention modules have appreciable robustness in comparison

to original ResNet, but do not always maintain their original 224x224 performance, and the best performing module (FCA) has a 0.5% lesser performance than TD-models at the best setting.

## 4.2. Attention visualization and weakly-supervised object localization

To better understand the workings of our proposed TD module, we utilize Grad-CAM maps [31] to visualize the model’s attention at each computation step for images drawn from the aforementioned validation sets. As shown in figure 6, we find that the model implicitly learns to shift its attention over computation steps. We conjecture that this imparts the model two important capabilities – one, choosing which object to “focus” on at each computational step when multiple objects (known to the model) are present and two, which feature to “focus” on at a given computational step when a more ambiguous or “difficult” object is present as the input. As an example of the first case, consider the second image input in fig. 6, wherein the model at its first computational step accurately locates a ‘vine snake’ to be present in the scene (which the original model gets incorrect) and then shifts its attention to the radiator. In contrast, in input five (of same fig. 6), the model iteratively attends to different features to make a more informed prediction. At its first computational step, it identifies water as a primary feature and has an initial prediction of a ‘water-ouzel’, but in the second computational step, it shifts its attention to the head of the bird and consequently predicts the correct category – ‘goldfinch’. In comparison, the original Resnet50’s prediction (‘water-ouzel’) is based on a less selective and conjoined feature map of the bird and water.

To quantitatively assess the model’s attention capabil-

Model	ImageNet (V1)	
	Top1	Top5
ResNet50	57.04	68.67
ResNet101	58.54	69.86
ResNet50 + SE	56.62	67.88
ResNet50 + CBAM	58.91	70.54
ResNet50 + ECA	56.94	68.38
ResNet50 + FCA-TS	56.88	67.86
ResNet50 + TDjoint (t=2, m=1)	61.55	72.10
ResNet50 + TDtop (t=2, m=3)	<b>61.97</b>	<b>72.37</b>

Table 3. Weakly supervised object localization accuracy (%) on ImageNet (V1). TD models and CBAM that incorporate spatial attention increase performance of ResNet50 while purely channel attention methods reduce performance.

ity and resulting enhancement in feature selectivity, we evaluate it on weakly supervised ImageNet-1k localization challenge [10], which requires models to provide bounding boxes in addition to classification labels. For all models, we follow the same strategy as [31] to generate bounding boxes for output predicted classes, and report top-1 and top-5 localization accuracy on ImageNet-V1 in table 3. We find that both top performing TD configurations for object classification improve performance of ResNet50, with TD-top(t=2,m=3) notably increasing accuracy by 5%, and being 3% over the best baseline model – CBAM. Interestingly, channel attention methods of SE, ECA and FCA obtain worse performance than original ResNet50, suggesting strong importance of spatial attention in localization tasks. This also suggests the importance of top-down feedback introduced in this paper for obtaining better attention module.

### 4.3. Fine-grained and multi-label classification

To demonstrate the general applicability of our TD module across different tasks and assess its capability as a robust feature extractor, we evaluate its performance as a backbone for existing state-of-the-art methods for fine-grained classification and multi-label object classification. We use the “Weakly Supervised Data Augmentation” method [18] for fine-grained classification and “Asymmetric loss” method [29] for multi-label classification, and simply replace the model backbone in both methods with our pre-trained ImageNet-1k models. For fine-grained classification, we consider the Caltech-birds (CUB) and Stanford Dogs (Dogs) datasets and assess models on top-1 validation accuracy. For multi-label classification, we use MS-COCO and assess models on mAP and overall F1.

As shown in table 4, using TD models (denoted as TDj for TDjoint and TDt for TDtop) as a backbone leads to a notable improvement in all three tasks compared to a baseline ResNet50, specifically achieving 1.5% increment on CUB-200 and 2 points better mAP on MS-COCO. The relative improvement over CBAM, which performs purely feed-

Model (ResNet50)	CUB	Dogs	MS-COCO	
	Top1	Top1	mAP	F1-O
ResNet	88.26	85.97	77.58	75.45
SE	88.89	86.55	78.21	76.37
CBAM	89.37	86.98	79.17	77.15
FCA-TS	88.94	86.76	79.05	77.08
TDjoint (t=2, m=1)	89.61	87.08	<b>79.61</b>	<b>77.71</b>
TDtop (t=2, m=3)	<b>89.75</b>	<b>87.30</b>	79.56	77.62

Table 4. Performance of models as backbones for fine-classification (val. acc. % for CUB and Stanford Dogs) and multi-label classification (val. mAP and overall F1 for MS-COCO). TD-based ResNet50 backbones outperform baselines in both tasks.

forward channel and spatial attention, indicates a possible advantage in feedback-driven channel and spatial attention which may enable iterative task-specific refinement of constituent feature-maps within the backbone.

### 4.4. Ablative analysis of feedback computation

As indicated in Sec. 3, our proposed TD module has three primary factors – (i) choice of attention “TDjoint” or “TDtop” (ii) feedback distance ‘m’ and (iii) feedback steps ‘t’. Accordingly, we assess the impact of each factor by evaluating resulting module configurations on ImageNet classification. To evaluate factors (i) and (ii), we utilize ResNet50 as before and evaluate on ImageNet-1k classification. For factor (iii), we utilize relatively shallower models of MobileNetV3-large and ResNet18 and evaluate on a hierarchically reduced subset of ImageNet with 200 classes due to the high computation cost and training time associated with models with more than 3 feedback steps.

**Impact of feedback distance ‘m’ and “joint” vs “top” attention** As shown in the left plot of fig.7, we find that having a feedback distance of at least 1 is crucial to the performance of the module, i.e. the module requires distinct top and bottom feature maps, and applying top-down attention on the same single feature map as done in existing attention modules provides negligible performance benefit over the baseline ResNet50 while introducing high number of parameters. Next, performance is most improved at m=1 and m=3 for both TDjoint and TDtop. However, note this does not indicate that m=2 is an inferior option in general, as in the case of ResNet50, the bottom representation at m=2 is the bottleneck block input, which may not sufficiently benefit from attentional modulation. Finally, TDjoint(m=3) and TDjoint(m=1) are the top-2 performing modules configurations indicating the enhanced representation capacity offered in joint modelling of top and bottom feature maps. However, while TDjoint(m=3) has highest performance of 77.44%, it has 8% higher parameters than TDjoint(m=1) and TDtop(m=3). Hence, other variants are more preferable, and in particular, **we recognize TDjoint (t=2, m=1)**

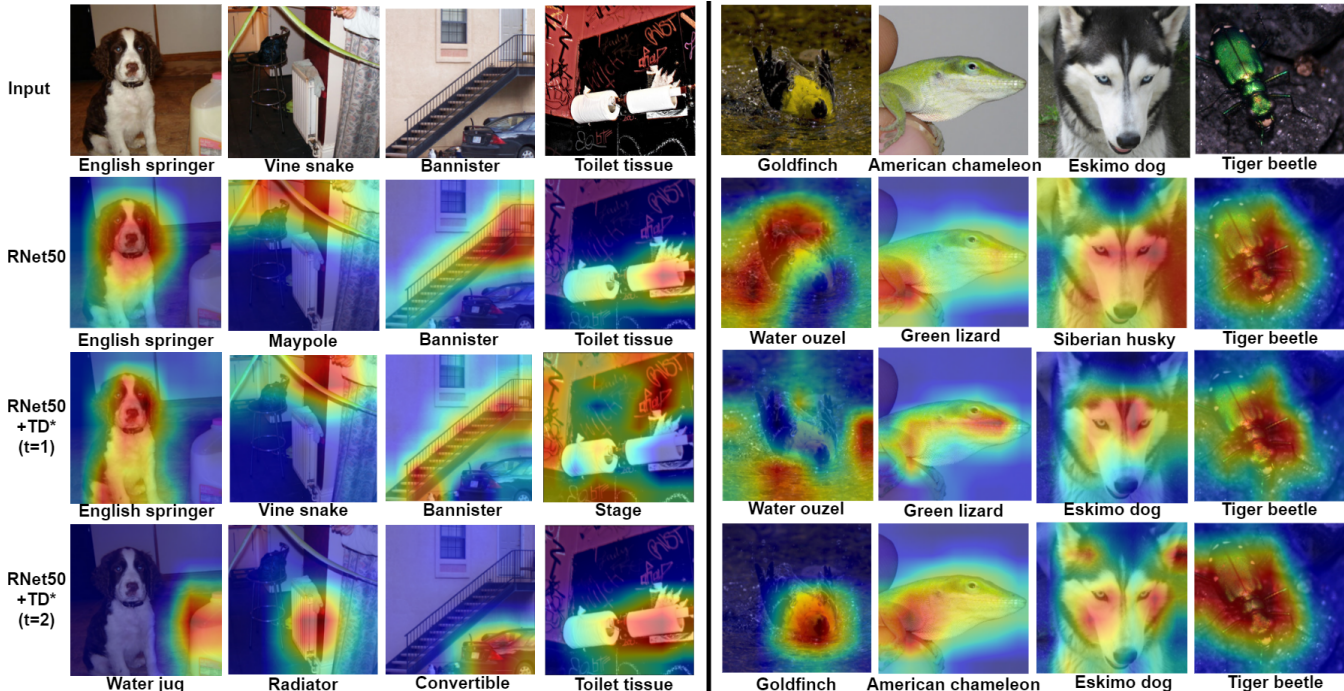


Figure 6. **Representative examples of “attention shifting” over computational steps of our model based on Grad-CAM analysis.** In the first 4 examples, the TD model iteratively attends to distinct objects and also has a more selective and complete feature activation at each computation step compared to original ResNet50. In the further 4 examples, it iteratively attends to relevant features for better discrimination of finer classes. See supplemental for more types of examples and code to try out on arbitrary examples.

as our primary top-down attention network.

**Impact of feedback steps ‘t’.** As shown in right plot of fig. 7, we find that for both ResNet18 and MobileNetV3, performance peaks at 2 feedback steps, and thereafter declines, but still retains higher performance than both a purely feedforward ( $t=1$ ) model and single feedback ( $t=2$ ) model. We conjecture that this decline at higher computation steps may be a result of possibly reduced value of gradients while training of the model (akin to “vanishing gradients”), leading to a less effective attentional searchlight at each feedback step. Note that in case of MobileNet, models with TD exhibit higher performance than the original model while having 15% lesser parameters and smaller model size, suggesting TD can be an effective component to integrate in models and methods for low-end devices.

## 5. Conclusions

We introduced a lightweight top-down attention module for CNNs that iteratively generates a “visual searchlight” to perform top-down channel and spatial attention of its constituent representations and outputs more selective feature activations. We performed extensive experiments with mainstream CNNs (ResNet and MobileNetV3), and showed that integrating our module outperforms baseline attention modules on large-scale object classification, fine-grained

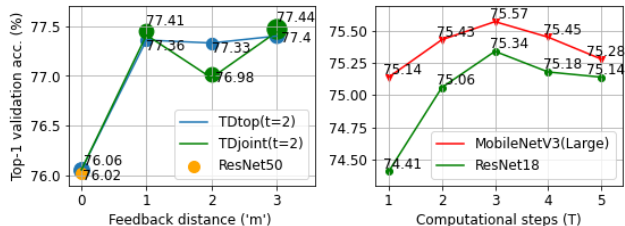


Figure 7. **Ablative analysis of our TD module.** Left: choice of attention operation (TDjoint or TDtop) and feedback distance ‘m’ (with ResNet50 on ImageNet-1k). Right: number of feedback steps ‘t’ (for MobileNetV3 large and ResNet18 on a hierarchically reduced subset of ImageNet with 200 classes).  $m=0$  and  $t=1$  refers to original feedforward models and circle sizes in left plot correspond to model size. Numerical reports in supplemental.

and multi-label classification. Further, we demonstrated the effectiveness of TD-models in remaining robust to increases in image resolutions during inference and also illustrated the emergent “attention shifting” behaviour and quantitatively assessed it on weakly supervised object localization, finding that it outputs significantly more precise localization maps. Finally, we performed ablative analysis to assess three primary factors of our module and determined TD-joint( $t=2$ ,  $m=1$ ) as our primary top-down attention network.



## References

- [1] Peter Anderson, Xiaodong He, Chris Buehler, Damien Teney, Mark Johnson, Stephen Gould, and Lei Zhang. Bottom-up and top-down attention for image captioning and visual question answering. In *Proceedings of the IEEE conference on computer vision and pattern recognition*, pages 6077–6086, 2018. 3
- [2] Jimmy Ba, Volodymyr Mnih, and Koray Kavukcuoglu. Multiple object recognition with visual attention. In *ICLR (Poster)*, 2015. 3
- [3] Irwan Bello, Barret Zoph, Ashish Vaswani, Jonathon Shlens, and Quoc V. Le. Attention augmented convolutional networks. In *Proceedings of the IEEE/CVF International Conference on Computer Vision (ICCV)*, October 2019. 1, 2
- [4] Wonmin Byeon, Thomas M Breuel, Federico Raue, and Marcus Liwicki. Scene labeling with lstm recurrent neural networks. In *Proceedings of the IEEE Conference on Computer Vision and Pattern Recognition*, pages 3547–3555, 2015. 3
- [5] Chunshui Cao, Xianming Liu, Yi Yang, Yinan Yu, Jiang Wang, Zilei Wang, Yongzhen Huang, Liang Wang, Chang Huang, Wei Xu, et al. Look and think twice: Capturing top-down visual attention with feedback convolutional neural networks. In *Proceedings of the IEEE international conference on computer vision*, pages 2956–2964, 2015. 3
- [6] Yue Cao, Jiarui Xu, Stephen Lin, Fangyun Wei, and Han Hu. Gcnet: Non-local networks meet squeeze-excitation networks and beyond. In *Proceedings of the IEEE/CVF International Conference on Computer Vision Workshops*, pages 0–0, 2019. 2
- [7] Long Chen, Hanwang Zhang, Jun Xiao, Liqiang Nie, Jian Shao, Wei Liu, and Tat-Seng Chua. Sca-cnn: Spatial and channel-wise attention in convolutional networks for image captioning. In *Proceedings of the IEEE conference on computer vision and pattern recognition*, pages 5659–5667, 2017. 3
- [8] Yunpeng Chen, Yannis Kalantidis, Jianshu Li, Shuicheng Yan, and Jiashi Feng. A<sup>2</sup>-nets: Double attention networks. In S. Bengio, H. Wallach, H. Larochelle, K. Grauman, N. Cesa-Bianchi, and R. Garnett, editors, *Advances in Neural Information Processing Systems*, volume 31. Curran Associates, Inc., 2018. 2
- [9] Francis Crick. Function of the thalamic reticular complex: the searchlight hypothesis. *Proceedings of the National Academy of Sciences*, 81(14):4586–4590, 1984. 2
- [10] Jia Deng, Wei Dong, Richard Socher, Li-Jia Li, Kai Li, and Li Fei-Fei. Imagenet: A large-scale hierarchical image database. In *2009 IEEE conference on computer vision and pattern recognition*, pages 248–255. Ieee, 2009. 5, 6, 7
- [11] Jianlong Fu, Heliang Zheng, and Tao Mei. Look closer to see better: Recurrent attention convolutional neural network for fine-grained image recognition. In *Proceedings of the IEEE conference on computer vision and pattern recognition*, pages 4438–4446, 2017. 3
- [12] Zilin Gao, Jiangtao Xie, Qilong Wang, and Peihua Li. Global second-order pooling convolutional networks. In *Proceedings of the IEEE/CVF Conference on Computer Vision and Pattern Recognition*, pages 3024–3033, 2019. 1, 2
- [13] Kaiming He, Xiangyu Zhang, Shaoqing Ren, and Jian Sun. Deep residual learning for image recognition. In *Proceedings of the IEEE conference on computer vision and pattern recognition*, pages 770–778, 2016. 1, 4, 5, 6
- [14] Andrew Howard, Mark Sandler, Grace Chu, Liang-Chieh Chen, Bo Chen, Mingxing Tan, Weijun Wang, Yukun Zhu, Ruoming Pang, Vijay Vasudevan, et al. Searching for mobilenetv3. In *Proceedings of the IEEE/CVF International Conference on Computer Vision*, pages 1314–1324, 2019. 5
- [15] Jie Hu, Li Shen, Samuel Albanie, Gang Sun, and Andrea Vedaldi. Gather-excite: Exploiting feature context in convolutional neural networks. In S. Bengio, H. Wallach, H. Larochelle, K. Grauman, N. Cesa-Bianchi, and R. Garnett, editors, *Advances in Neural Information Processing Systems*, volume 31. Curran Associates, Inc., 2018. 2
- [16] Jie Hu, Li Shen, and Gang Sun. Squeeze-and-excitation networks. In *Proceedings of the IEEE conference on computer vision and pattern recognition*, pages 7132–7141, 2018. 1, 2, 3, 5, 6
- [17] Peiyun Hu and Deva Ramanan. Bottom-up and top-down reasoning with hierarchical rectified gaussians. In *Proceedings of the IEEE Conference on Computer Vision and Pattern Recognition*, pages 5600–5609, 2016. 3
- [18] Tao Hu, Honggang Qi, Qingming Huang, and Yan Lu. See better before looking closer: Weakly supervised data augmentation network for fine-grained visual classification. *arXiv preprint arXiv:1901.09891*, 2019. 7
- [19] Aditya Khosla, Nityananda Jayadevaprakash, Bangpeng Yao, and Li Fei-Fei. Novel dataset for fine-grained image categorization. In *First Workshop on Fine-Grained Visual Categorization, IEEE Conference on Computer Vision and Pattern Recognition*, Colorado Springs, CO, June 2011. 5
- [20] Qianli Liao and Tomaso Poggio. Bridging the gaps between residual learning, recurrent neural networks and visual cortex. *arXiv preprint arXiv:1604.03640*, 2016. 4
- [21] Tsung-Yi Lin, Michael Maire, Serge Belongie, James Hays, Pietro Perona, Deva Ramanan, Piotr Dollár, and C Lawrence Zitnick. Microsoft coco: Common objects in context. In *European conference on computer vision*, pages 740–755. Springer, 2014. 5
- [22] Jiang-Jiang Liu, Qibin Hou, Ming-Ming Cheng, Changhu Wang, and Jiashi Feng. Improving convolutional networks with self-calibrated convolutions. In *Proceedings of the IEEE/CVF Conference on Computer Vision and Pattern Recognition*, pages 10096–10105, 2020. 1, 2
- [23] Volodymyr Mnih, Nicolas Heess, Alex Graves, and koray kavukcuoglu. Recurrent models of visual attention. In Z. Ghahramani, M. Welling, C. Cortes, N. Lawrence, and K. Q. Weinberger, editors, *Advances in Neural Information Processing Systems*, volume 27. Curran Associates, Inc., 2014. 3
- [24] Jongchan Park, Sanghyun Woo, Joon-Young Lee, and In So Kweon. BAM: bottleneck attention module. In *British Machine Vision Conference 2018, BMVC 2018, Newcastle, UK, September 3-6, 2018*, page 147. BMVA Press, 2018. 2
- [25] Adam Paszke, Sam Gross, Francisco Massa, Adam Lerer, James Bradbury, Gregory Chanan, Trevor Killeen, Zeming

- Lin, Natalia Gimelshein, Luca Antiga, Alban Desmaison, Andreas Kopf, Edward Yang, Zachary DeVito, Martin Raison, Alykhan Tejani, Sasank Chilamkurthy, Benoit Steiner, Lu Fang, Junjie Bai, and Soumith Chintala. Pytorch: An imperative style, high-performance deep learning library. In H. Wallach, H. Larochelle, A. Beygelzimer, F. d'Alché-Buc, E. Fox, and R. Garnett, editors, *Advances in Neural Information Processing Systems*, volume 32. Curran Associates, Inc., 2019. 5
- [26] Pedro Pinheiro and Ronan Collobert. Recurrent convolutional neural networks for scene labeling. In *International conference on machine learning*, pages 82–90. PMLR, 2014. 3
- [27] Zequn Qin, Pengyi Zhang, Fei Wu, and Xi Li. Fcanet: Frequency channel attention networks. In *Proceedings of the IEEE/CVF International Conference on Computer Vision*, pages 783–792, 2021. 1, 2, 5, 6
- [28] Benjamin Recht, Rebecca Roelofs, Ludwig Schmidt, and Vaishaal Shankar. Do imagenet classifiers generalize to imagenet? In *International Conference on Machine Learning*, pages 5389–5400. PMLR, 2019. 5, 6
- [29] Tal Ridnik, Emanuel Ben-Baruch, Nadav Zamir, Asaf Noy, Itamar Friedman, Matan Protter, and Lihi Zelnik-Manor. Asymmetric loss for multi-label classification. In *Proceedings of the IEEE/CVF International Conference on Computer Vision*, pages 82–91, 2021. 7
- [30] Abhijit Guha Roy, Nassir Navab, and Christian Wachinger. Recalibrating fully convolutional networks with spatial and channel “squeeze and excitation” blocks. *IEEE transactions on medical imaging*, 38(2):540–549, 2018. 2, 4
- [31] Ramprasaath R Selvaraju, Michael Cogswell, Abhishek Das, Ramakrishna Vedantam, Devi Parikh, and Dhruv Batra. Grad-cam: Visual explanations from deep networks via gradient-based localization. In *Proceedings of the IEEE international conference on computer vision*, pages 618–626, 2017. 6, 7
- [32] Hugo Touvron, Andrea Vedaldi, Matthijs Douze, and Herve Jegou. Fixing the train-test resolution discrepancy. In H. Wallach, H. Larochelle, A. Beygelzimer, F. d'Alché-Buc, E. Fox, and R. Garnett, editors, *Advances in Neural Information Processing Systems*, volume 32. Curran Associates, Inc., 2019. 2, 4, 5
- [33] Anne M Treisman and Garry Gelade. A feature-integration theory of attention. *Cognitive psychology*, 12(1):97–136, 1980. 2
- [34] Fei Wang, Mengqing Jiang, Chen Qian, Shuo Yang, Cheng Li, Honggang Zhang, Xiaogang Wang, and Xiaoou Tang. Residual attention network for image classification. In *Proceedings of the IEEE conference on computer vision and pattern recognition*, pages 3156–3164, 2017. 2
- [35] Qilong Wang, Banggu Wu, Pengfei Zhu, Peihua Li, Wangmeng Zuo, and Qinghua Hu. Eca-net: efficient channel attention for deep convolutional neural networks, 2020 ieee. In *CVF Conference on Computer Vision and Pattern Recognition (CVPR). IEEE*, 2020. 1, 2, 5, 6
- [36] P. Welinder, S. Branson, T. Mita, C. Wah, F. Schroff, S. Belongie, and P. Perona. Caltech-UCSD Birds 200. Technical Report CNS-TR-2010-001, California Institute of Technology, 2010. 5
- [37] Sanghyun Woo, Jongchan Park, Joon-Young Lee, and In So Kweon. Cbam: Convolutional block attention module. In *Proceedings of the European conference on computer vision (ECCV)*, pages 3–19, 2018. 1, 2, 4, 5, 6
- [38] Kelvin Xu, Jimmy Ba, Ryan Kiros, Kyunghyun Cho, Aaron Courville, Ruslan Salakhudinov, Rich Zemel, and Yoshua Bengio. Show, attend and tell: Neural image caption generation with visual attention. In *International conference on machine learning*, pages 2048–2057. PMLR, 2015. 3
- [39] Jianwei Yang, Zhile Ren, Chuang Gan, Hongyuan Zhu, Ji Lin, and Devi Parikh. Cross-channel communication networks. 2019. 2
- [40] Zichao Yang, Xiaodong He, Jianfeng Gao, Li Deng, and Alex Smola. Stacked attention networks for image question answering. In *Proceedings of the IEEE conference on computer vision and pattern recognition*, pages 21–29, 2016. 3
- [41] Amir R Zamir, Te-Lin Wu, Lin Sun, William B Shen, Bertram E Shi, Jitendra Malik, and Silvio Savarese. Feedback networks. In *Proceedings of the IEEE conference on computer vision and pattern recognition*, pages 1308–1317, 2017. 3
- [42] Matthew D Zeiler and Rob Fergus. Visualizing and understanding convolutional networks. In *European conference on computer vision*, pages 818–833. Springer, 2014. 3, 4
- [43] Mengmi Zhang, Claire Tseng, and Gabriel Kreiman. Putting visual object recognition in context. In *Proceedings of the IEEE/CVF Conference on Computer Vision and Pattern Recognition*, pages 12985–12994, 2020. 3